Electronic Supplementary Material (ESI) for Journal of Materials Chemistry A.

Supporting Information

In-situ formed VOOH nanosheet arrays anchored on $Ti_3C_2T_x$ MXene as a highly efficient and robust synergistic electrocatalyst for boosting water oxidation and reduction

Liang Yan,*[a,b] Xuanwei Chen,[a] Xiaojun Liu,[a] Liping Chen[a] and Bing Zhang[c]

[a] *School of Chemistry and Materials Engineering, Huizhou University, No. 46 Yanda Road, Huizhou, 516007, China.*

[b] *Guangdong Provincial Key Laboratory for Electronic Functional Materials and Devices, Huizhou University, No. 46 Yada Road, Huizhou, 516007, China.*

[c] *School of Materials and Energy, Guangdong University of Technology, Guangzhou Higher EducationMega Center, No. 100 Waihuan Xi Road, Guangzhou, 510006, China.*

* *Corresponding author.*

E-mail address: yanliang@hzu.edu.cn

Experimental Section

Chemicals and Materials: Ammonium vanadate (NH_4VO_3), hydrazine hydrate ($N_2H_4 \cdot H_2O$), hydrochloric acid (HCl), lithium fluoride (LiF, 99%), and anhydrous ethanol (C_2H_5OH, >99.5%) were obtained from Aladdin Reagents Ltd. The commercial Pt/C (20 wt% Pt on Vulcan XC-72R) was purchased from Johnson Mattey, while commercial IrO_2 was purchased from Alfa Aesar. Nafion (5 wt%) was purchased from Sigma-Aldrich. Carbon paper (CP, #60, 0.19 mm in thickness) was bought from Toray Industries, Inc. and washed sequentially with acetone, ethanol and deionized (DI) water before use. All the chemicals were used as received without further purification.

Preparation of $Ti_3C_2T_x$ MXene nanosheets: Ti_3AlC_2 powders (> 99.5 wt % purity) were bought from 11 Technology Co., Ltd. $Ti_3C_2T_x$ MXene nanosheets were synthesized via etching the Ti_3AlC_2 powder with HF. Typically, 1.0 g of LiF was dissolved in 20.0 mL of 9.0 M HCl solution and stirred for 30 min, then 1.0 g of Ti_3AlC_2 powder was slowly added into the aforementioned solution and the mixed solution was kept stirring at 35 °C for 24 h. Afterward, the resulting suspension washed with DI water for several times until the neutral pH (≥6) was obtained. The collected powder was ultrasonicated in 200 mL of DI water for 1 h under continuous Ar purging. The obtained aqueous solution containing monolayer or few-layer $Ti_3C_2T_x$ MXene nanosheets was centrifuged at 3500 rpm for 1 h and the supernatant was freeze-dried to obtain $Ti_3C_2T_x$ MXene powder.

Synthesis of VOOH nanosheet arrays on $Ti_3C_2T_x$ MXene nanosheets: In a typical synthesis, 30 mg of $Ti_3C_2T_x$ MXene powder was first dispersed in 15 mL of deoxygenated DI water by ultrasonic treatment 1 h under the protection of Ar. Meantime, 2 mM of NH_4VO_3 was dissolved in 20 mL of DI water to obtain a homogeneous solution. Then, the obtained $Ti_3C_2T_x$ MXene suspension was added into the NH_4VO_3 solution under stirring, and the mixed solution was keeping stirred at room temperature for 1 h under the protection of Ar. HCl (1 mL 1 M) and $N_2H_4 \cdot H_2O$ (1 mL) were then dropwise added in turn to the above mixture solution and continuous magnetic stirring for 30 min under the protection of Ar. Afterwards, the obtained solution was poured into a 50 mL Teflon-lined stainless-steel autoclave and reacted at 160 °C for 8 h. After cooling down to room temperature, the resulting products were thoroughly washed with deoxygenated DI water and ethanol several times and then freeze-dried overnight. Finally, the obtained VOOH/$Ti_3C_2T_x$ MXene (164.4 mg) was collected and then stored at 0 °C in Ar-filled bottles before use. For comparison, bare VOOH was synthesized using a similar procedure to that of VOOH/$Ti_3C_2T_x$ MXene except that no $Ti_3C_2T_x$ MXene was added.

Material characterizations: The XRD patterns were recorded on a D8 Advance X-ray powder diffractometer with Cu Kα radiation ($\lambda = 1.54$ Å) as the X-ray source. Surface Morphology and microstructure of the samples were characterized by field emission scanning electron microscopy (FESEM, Hitachi SU8220) and field emission transmission electron microscope (FETEM, FEI Talos F200S). Surface chemistry and elemental composition were characterized by X-ray photoelectron spectroscopy (XPS, Thermo Fisher ESCALAB 250Xi) with Al Kα radiation. Raman spectra were carried out on a LabRAM HR Evolution Raman microscope with 532 nm wavelength excitation laser. N_2 adsorption-desorption isotherms were measured by the Brunauer-Emmett-Teller (BET, Micrometrics ASAP 2460) method. Weight ratio of V and Ti elements in the sample were analyzed by inductively coupled plasma optical emission spectroscopy (ICP-OES, Optima 4300DV).

Electrochemical Measurements: All electrochemical measurements were performed on a PGSTAT302N potentiostat/galvanostat (Metrohm Autolab, Netherlands) workstation equipped with a three-electrode setup. A glassy-carbon (GC) rotating disk electrode (RDE) (d = 5.0 mm) was used as working electrode, while a reversible hydrogen electrode (RHE) and a graphite rod were used as the reference and counter electrodes, respectively. First, the catalyst ink was prepared by ultrasonically dispersing the mixture of the catalyst (5 mg), ethanol (500 μL), deionized water (490 μL) and Nafion (10 μL, 5 wt%) for 30 min to form a uniform suspension. Next, 10 μL of the catalyst dispersion was then carefully dropped onto a GC electrode and dried under atmospheric conditions. For comparison, the commercial IrO_2 and Pt/C (20%) with the similar mass loading were also prepared as benchmark OER and HER catalysts, respectively. Prior to the measurement, the electrolyte (1.0 M KOH) was purged with high purity O_2 or Ar flow for 30 min and maintained during the measurement to ensure continuous gas saturation. Linear sweep voltammograms (LSV) for both OER and HER were measured at a scan rate of 5 mV s^{-1} and corrected with 95% iR compensation. The electrochemical double-layer capacitance (C_{dl}) was measured from cyclic voltammogram method in a potential range without apparent faradaic process at various scan rates ranging from 10 to 100 mV s^{-1}. Electrochemical impedance spectra (EIS) measurements were carried out over a frequency range from 0.1 Hz to 100 kHz by applying an AC potential with 5 mV amplitude. The long-term stability was recorded by a chronopotentiometry measurement at a constant current density of ±10 mA cm^{-2}. The overall water splitting measurement was carried out in a two-electrode system using the VOOH/$Ti_3C_2T_x$ MXene as a bifunctional catalyst with a loading of 2 mg cm^{-2} on CP as both the cathode and anode in Ar-saturated 1.0 M KOH. For comparison, the physical mixture of VOOH and $Ti_3C_2T_x$ MXene (denoted as VOOH@$Ti_3C_2T_x$ MXene) was prepared by mechanically mixing VOOH powders (134.4 mg) and $Ti_3C_2T_x$ MXene (30 mg) in an argon-filled glovebox using a mortar at room temperature. The catalytic performance of VOOH@$Ti_3C_2T_x$ MXene was also tested for better comparison.

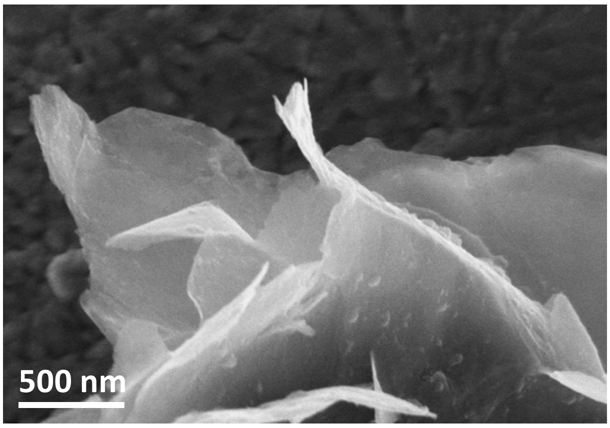

Figure S1. SEM image of $Ti_3C_2T_x$ Mxene.

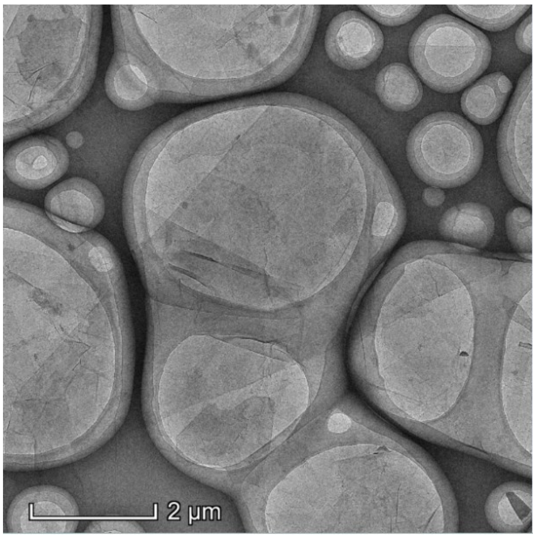

Figure S2. TEM image of $Ti_3C_2T_x$ Mxene.

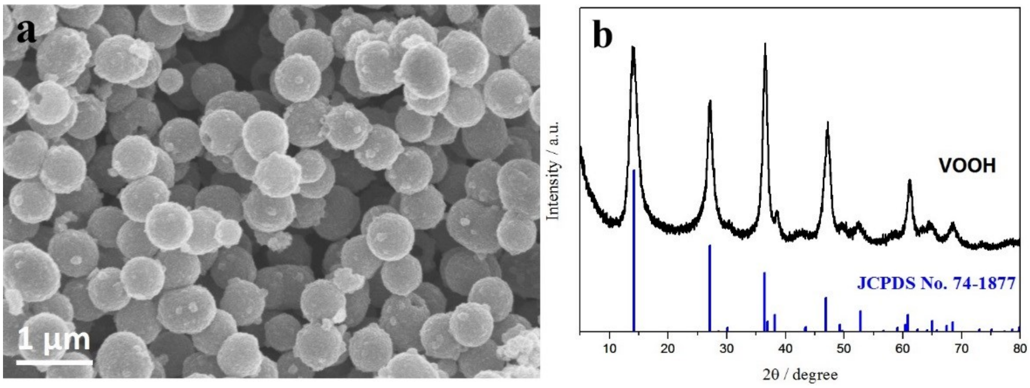

Figure S3. (a) SEM image and (b) the XRD pattern of VOOH.

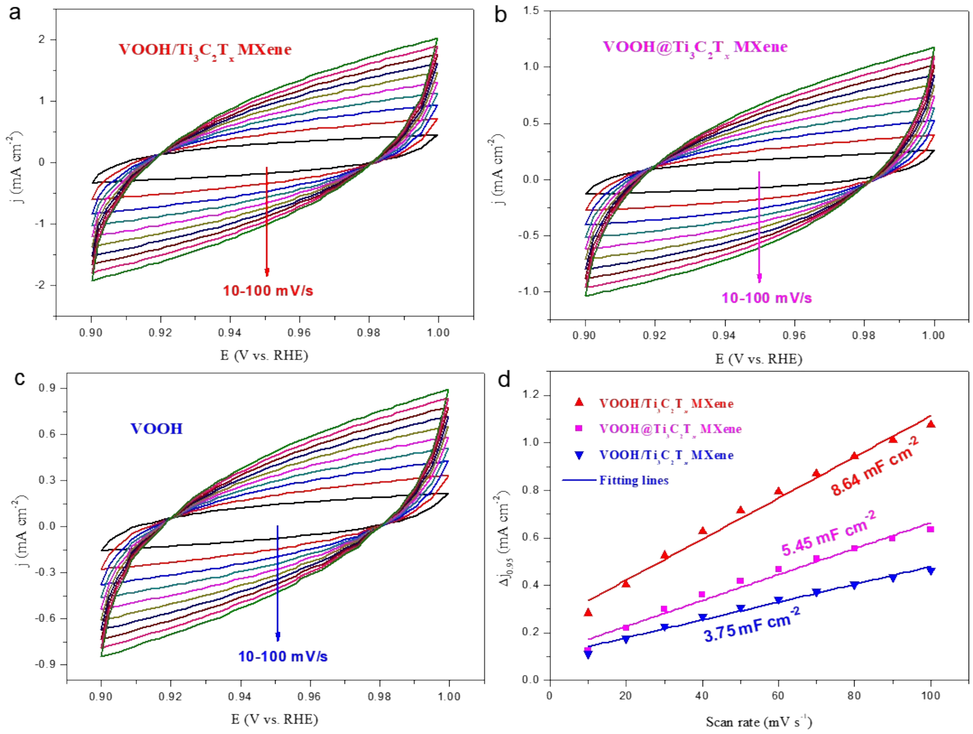

Figure S4. CV curves for (a) VOOH/$Ti_3C_2T_x$ Mxene, (b) VOOH@$Ti_3C_2T_x$ Mxene and (c) VOOH at different scan rates (10-100 mV s^{-1}). (c) The C_{dl} value of VOOH/$Ti_3C_2T_x$ Mxene, VOOH@$Ti_3C_2T_x$ Mxene and VOOH.

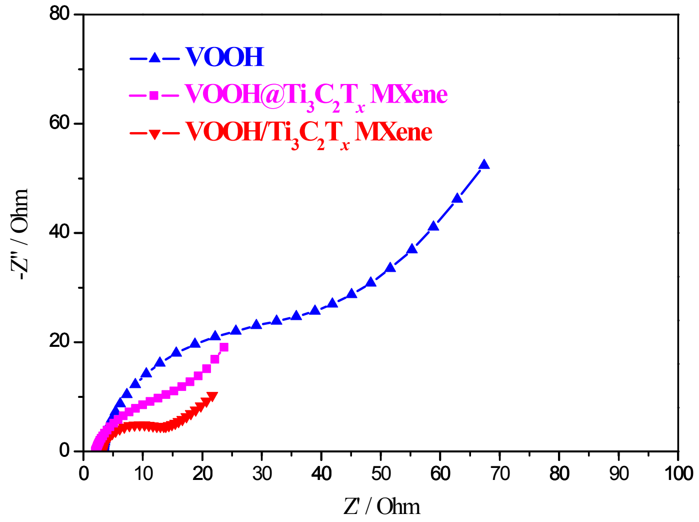

Figure S5. EIS Nyquist Plots of VOOH, VOOH@Ti$_3$C$_2$T$_x$ Mxene and VOOH/Ti$_3$C$_2$T$_x$ Mxene for OER.

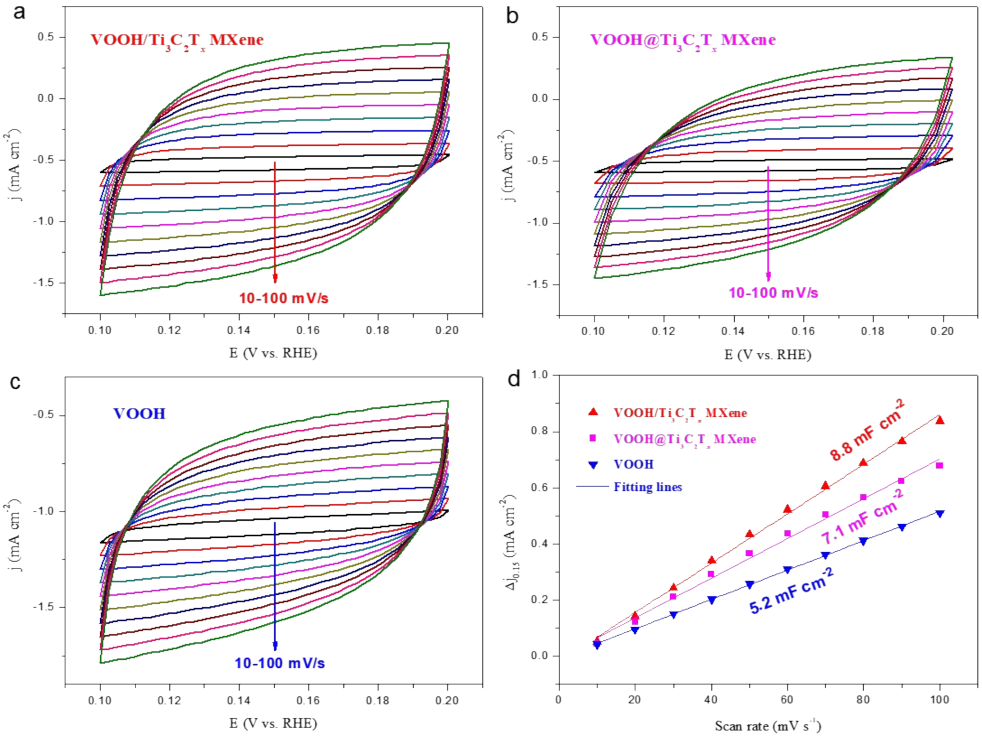

Figure S6. CV curves for (a) VOOH/$Ti_3C_2T_x$ Mxene, (b) VOOH@$Ti_3C_2T_x$ Mxene and (c) VOOH at different scan rates (10-100 mV s^{-1}). (c) The C_{dl} value of VOOH/$Ti_3C_2T_x$ Mxene, VOOH@$Ti_3C_2T_x$ Mxene and VOOH.

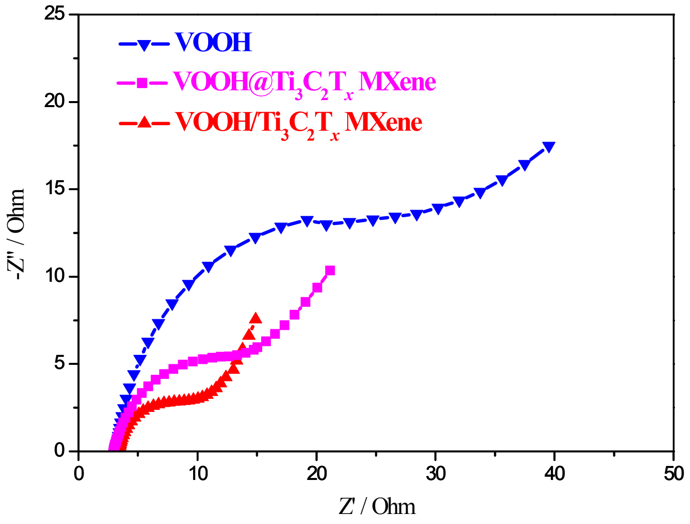

Figure S7. EIS Nyquist Plots of VOOH, VOOH@$Ti_3C_2T_x$ Mxene and VOOH/$Ti_3C_2T_x$ Mxene for HER.

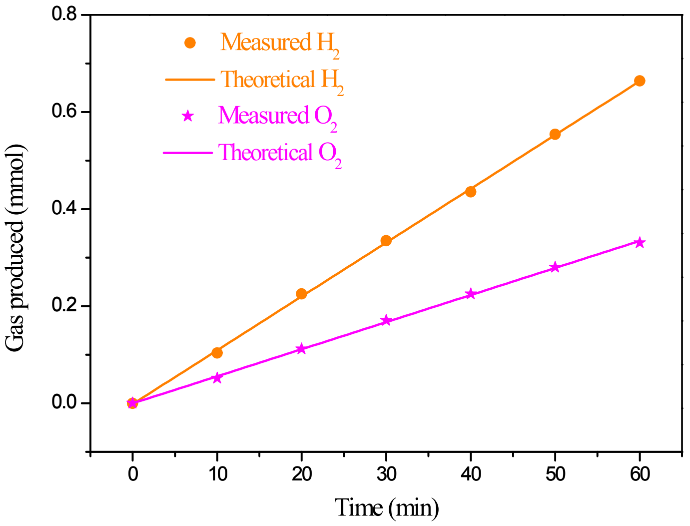

Figure S8. Amount of gas theoretically calculated and experimentally measured vs. time for overall water splitting of VOOH/$Ti_3C_2T_x$ Mxene.

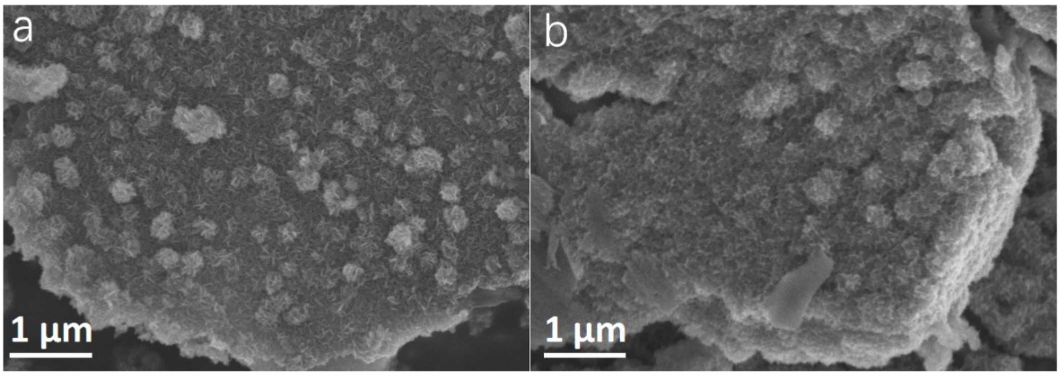

Figure S9. SEM images of VOOH/$Ti_3C_2T_x$ Mxene after (a) HER and (b) OER measurements.

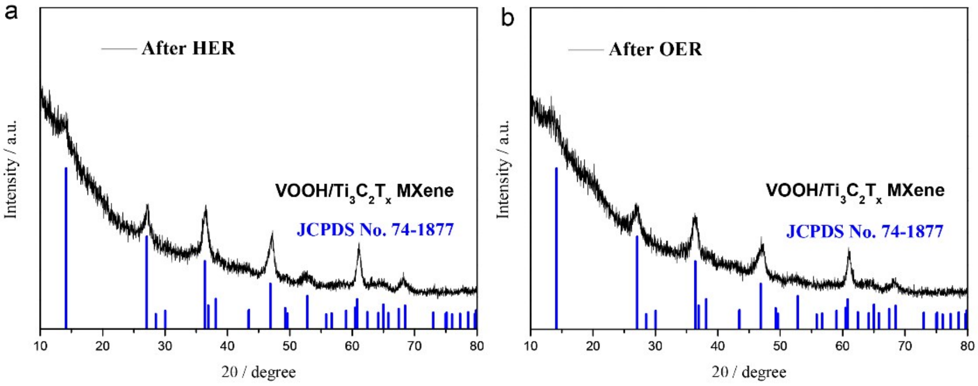

Figure S10. XRD pattern of VOOH/$Ti_3C_2T_x$ Mxene after (a) HER and (b) OER measurements.

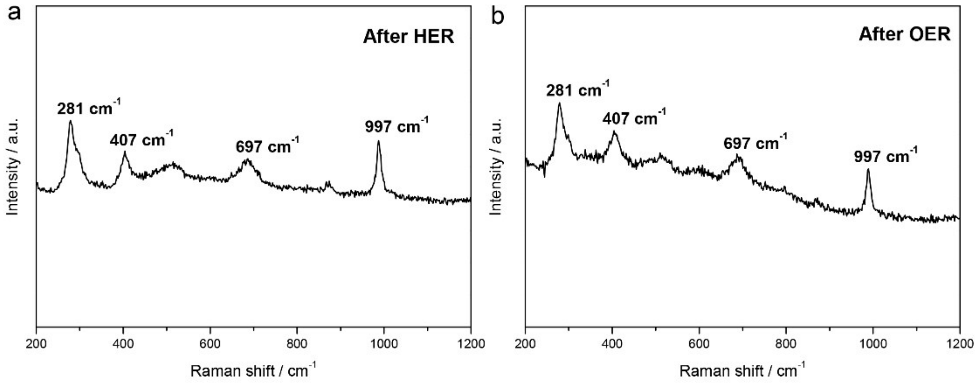

Figure S11. Raman spectra of VOOH/$Ti_3C_2T_x$ Mxene after (a) HER and (b) OER measurements.

Table S1. A comparison of OER performances of VOOH/$Ti_3C_2T_x$ Mxene with recently reported electrocatalysts in 1.0 M KOH.

Catalyst	η (mV) at 10 mA cm^{-2}	Tafel slope mV dec^{-1}	Reference
γ-CoOOH nanosheet	300	38	*Angew. Chem. Int. Ed.* **2015**, *54*, 8722
$NiPS_3$@NiOOH	350^a	80	*ACS Catal.* **2017**, *7*, 229
Fe-CoOOH/G	330	37	*Adv. Energy Mater.* **2017**, *7*, 1602148
VOOH	270	68	*Angew. Chem. Int. Ed.* **2017**, *56*, 573
F-CoOOH/NF	270	54	*Angew. Chem. Int. Ed.* **2018**, *57*, 15471
Zn-CoOOH/NF	270	44	*Nano Energy* **2018**, *53,* 144
δ-FeOOH NSs/NF	265	68	*Adv. Mater.* **2018**, *30*, 1803144
Co-Bi/$Ti_3C_2T_x$ MXene	250	53	*ChemSusChem* **2018**, *11*, 3758
BP QDs/MXene	360	64.3	*J. Mater. Chem. A* **2018**, *6,* 21255
Co_3O_4 QDs/MXene	340	63.97	*Chem. Commun.* **2019**, *55*, 1237
CoP/Ti_3C_2 MXene	230	50	*J. Mater. Chem. A* **2019**, *7*, 27383
NiFe-LDH/MXene/NF	229	43	*Nano Energy* **2019**, *63*, 103880
$Ti_3C_{1.6}N_{0.4}$	450	216.4	*Nanoscale Adv.* **2020**, *2*, 1187
$M_3OOH@V_4C_3T_x$ MXene	275.2	51.4	*InfoMat.* **2020**, *2*, 1
FeOOH NSs/Ti_3C_2 MXene	400	95	*ChemistrySelect* **2020**, *5*, 1890
Co_3O_4/MXene	300	118	*Sci. Bull.* **2020**, *65*, 460
FeCo-LDH/MXene	268	85	*ChemNanoMat* **2020**, *6*, 154
VOOH/$Ti_3C_2T_x$ Mxene	238	81.6	This work

a: 0.1 M KOH

Table S2. A comparison of HER performances of VOOH/$Ti_3C_2T_x$ Mxene with recently reported electrocatalysts in 1.0 M KOH.

Catalyst	η (mV) at 10 mA cm^{-2}	Tafel slope mV dec^{-1}	Reference
VOOH	164	104	*Angew. Chem. Int. Ed.* **2017**, 56, 573
Cu@CoFe LDH	171	36.4	*Nano Energy* **2017**, *41*, 327
BP QDs/MXene	190	83	*J. Mater. Chem. A* **2018**, *6,* 21255
CoP@3D Ti_3C_2-MXene	168	58	*ACS Nano* **2018**, *12*, 8017
Co-Fe oxyphosphide	180	62	*Adv. Sci.* **2019**, *6*, 1900576
FeCoNi (Oxy)hydroxide	150	107	*Adv. Energy Mater.* **2019**, *9*, 1901312
NiS_2/V-MXene	179	85	*J. Catal.* **2019**, *375*, 8
CoP/Ti_3C_2 MXene	113	57	*J. Mater. Chem. A* **2019**, *7*, 27383
NiFe-LDH/MXene/NF	132	70	*Nano Energy* **2019**, *63*, 103880
VS_2@V_2C MXene	164	47.6	*Nanoscale* **2020**, *12*, 6176
Co^{3+}@3D-Nb_2CT_x MXene	236	123	*Adv. Sci.* **2020**, *7*, 1903680
MoS_2@Mo_2CT_x	176	207	*CrystEngComm* **2020**, *22*, 1395
IrCo@ac-Ti_3C_2	135	56	*ChemSusChem* **2020**, *13*, 945
2.5% Pt@2D MXene	103	52	*Adv. Funct. Mater.* **2020**, *30*, 1910028
VOOH/$Ti_3C_2T_x$ Mxene	100	81.8	This work

Table S3. A comparison of VOOH/$Ti_3C_2T_x$ Mxene with recently reported bifunctional electrocatalysts in the performance for overall water splitting.

Catalyst	Potential (V) at 10 mA cm^{-2}	Reference
VOOH	1.62	*Angew. Chem. Int. Ed.* **2017**, 56, 573
δ-FeOOH NSs/NF	1.62	*Adv. Mater.* **2018**, *30*, 1803144
BP QDs/MXene	1.78	*J. Mater. Chem. A* **2018**, *6,* 21255
$Ni_{0.7}Fe_{0.3}PS_3$@MXene || $Ni_{0.9}Fe_{0.1}PS_3$@MXene	1.65	*Adv. Energy Mater.* **2018**, *8*, 1801127
CoP@3D Ti_3C_2-MXene	1.565	*ACS Nano* **2018**, *12*, 8017
CoP/MXene	1.56	*J. Mater. Chem. A* **2019**, *7*, 27383
γ-CrOOH/NF	1.56	*Inorg. Chem.* **2019**, *58*, 4014
NiFe-LDH/MXene/NF	1.51	*Nano Energy* **2019***, 63,* 103880
1T/2H $MoSe_2$/MXene	1.64	*Electrochim. Acta* **2019**, *326*, 134976
Ni_3S_2@MoS_2/FeOOH	1.57	*Appl. Catal. B: Environ*. **2019***, 244,* 1004
FeOOH/Ni_3N/CC	1.58	*Appl. Catal. B: Environ*. **2020***, 269,* 118600
$Ni_{0.8}Fe_{0.2}$-AHNA||Ni	1.41	*Energy Environ. Sci.* **2020**, *13*, 86
VOOH/$Ti_3C_2T_x$ Mxene	1.579	This work